Angular dependence of ferromagnetic resonance as indicator of the nature of magnetoelectric coupling in ferromagnetic-ferroelectric heterostructures

A. Sukhov,[1] C.-L. Jia,[2] L. Chotorlishvili,[1] P. P. Horley,[3] D. Sander,[4] and J. Berakdar[1]
[1]*Institut für Physik, Martin-Luther-Universität Halle-Wittenberg, 06120 Halle/Saale, Germany*
[2]*Key Laboratory for Magnetism and Magnetic Materials of the Ministry of Education, Lanzhou University, 730000, China*
[3]*Centro de Investigacion en Materiales Avanzados (CIMAV S.C.), Chihuahua/Monterrey, Mexico*
[4]*Max Planck Institute of Microstructure Physics, 06120 Halle/Saale, Germany*
(Received 23 September 2014; revised manuscript received 28 October 2014; published 31 December 2014)

We investigate theoretically how ferromagnetic resonance (FMR) in a multiferroic heterostructure provides quantitative information on multiferroic coupling. In particular, we analyze the asymmetry of the angular dependence of FMR on the direction of resonance magnetic fields as experimentally reported for $Co/BaTiO_3$ [Jedrecy *et al.*, Phys. Rev. B **88**, 121409(R) (2013)] and for permalloy/$Pb(MgNb)O_3$-$PbTiO_3$ [Nan *et al.*, Sci. Rep. **4**, 3688 (2014)]. Based on both analytical expressions for the dependence of FMR on the magnetic-field orientation and full numerical simulations which account for mutually coupled polarization **P** and magnetization **M** dynamics, we conclude that it is the linear magnetoelectric coupling in **P** and **M** originating from spin-dependent screening that leads to the experimentally observed asymmetry in FMR angular behavior. This suggests that angular resolved FMR is well suited to quantify the type and the strength of magnetoelectric coupling. In addition, we predict a pronounced thickness dependence of the resonance asymmetries and show how the FMR angular asymmetry can be tuned by an external static electric field. The possibility to observe electric-field-assisted FMR in the absence of an external static magnetic field is also discussed.

DOI: 10.1103/PhysRevB.90.224428 PACS number(s): 75.78.Fg, 75.85.+t, 76.50.+g

I. INTRODUCTION

Much research has been devoted to multiferroic (MF) materials [1–4] over recent decades also due to the promise of realizing qualitatively new device concepts based on electric/magnetic control of magnetism/ferroelectricity via magnetoelectric (ME) coupling [5–9]. For instance, this type of control of magnetization offers several advantages as compared to conventional approaches utilizing current-induced magnetic fields [10–12] or spin-polarized currents [13–17]. Magnetoelectric coupling appears favorable in these applications as it promises a superior energy efficiency and less Joule heating. A disadvantage is however the notoriously small strength of ME coupling in single-phase MFs [2,18] and the lack of full and thorough understanding of its origin. Also, strategies to control the coupled ferroelectric (FE) and ferromagnetic (FM) dynamic response [19], which is an important issue for understanding the formation of FE or FM domains [20], have yet to be established.

Some remedies of these conceptual challenges are expected from appropriately engineered composite MFs [21,22] with high room-temperature ME effects and large FE- and FM-order parameters. Indeed, heterostructure MF spintronic tunnel junctions were demonstrated experimentally, e.g., Refs. [7,9], and coupled MF excitations were studied [23].

In this contribution we focus on a particular type of MF excitations, namely, ferromagnetic resonance (FMR) in a composite MF, and we elucidate the FMR signal dependence on ME coupling and on a possibly applied electric field. Special attention is paid to the symmetry of the angular dependence of FMR on the direction of magnetic resonance fields reported recently in Refs. [24,25]. In Ref. [24] a nanometer thin polycrystalline Co film was deposited on a single-crystalline $BaTiO_3(001)$ (BTO) layer with a tetragonal phase and grown on a $SrTiO_3(001)$ substrate. This structure showed an unexpectedly strong out-of-plane remanent magnetization and a pronounced asymmetry of the angular dependence of resonance fields in FMR [$B_{res}(\theta_B)$]. This asymmetry of the resonance field for magnetization along the sample normal at 0° and 180° amounts to 0.14 T (cf. schematics of Fig. 1). The authors of Ref. [24] ascribe this finding to the magnetoelectric coupling at the $Co/BaTiO_3$ interface. A detailed analysis and simulations of this asymmetry including the contributions of other factors, such as other types of coupling mechanisms, and thickness dependence are still missing. As an established sensitive probe, FMR would be a valuable tool for MF research if one can relate the FMR signal and in particular its angular dependence to the details of ME coupling.

Here we present a systematic analysis of FMR on a MF composite supported by comprehensive numerical simulations, and we discuss the result in view of recent experiments. We note that recently a microscopic mechanism has been presented [26] for the ME coupling, that leads to ME coupling that is linear in **P** and **M**. Its range is on the order of the spin diffusion length (38 ± 12 nm for bulk Co [27]), and it extends in the vicinity of the FE/FM interface. The essence of the mechanism is that on the FM side a noncollinear magnetic order is formed with an effective (fictitious) electric field that screens the interfacial polarization on the FE side. In Ref. [26] it was also discussed why this linear ME mechanism is relevant for the permalloy/PMN-PT ($0.71Pb(Mg_{1/3}Nb_{2/3}O_3)$-$0.29PbTiO_3$) [25]. Hence, the phenomena inferred below for the FMR characteristics as a consequence of the linear ME coupling apply also to permalloy/PMN-PT. A key point of this new mechanism in view of the FMR experiments discussed here is that the ME coupling is operational in the FM on the scale of nanometers away from the interface. Thus, it is not strictly confined to the interface layer. As a consequence we expect indications of ME coupling in FMR even for nanometer-thick samples. For the macroscopic FM part, the effect of ME on FMR is expected to

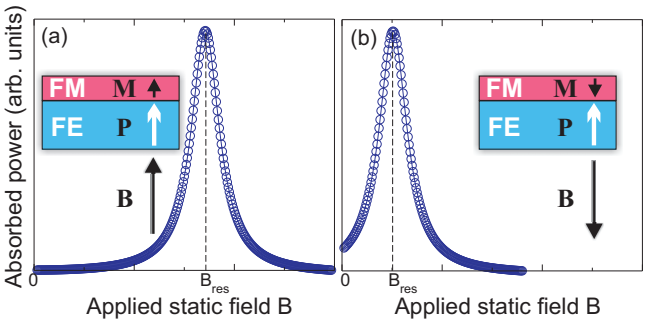

FIG. 1. (Color online) Schematic of the effect of finite ME coupling on FMR spectra when: (a) The net magnetization **M** and the magnetic static field **B** are both aligned parallel to the electric polarization **P** and (b) are both antiparallel with the direction of **P**. Note, that the resonance field $B_{\rm res}$ differs for parallel and antiparallel orientations between **M** and **P**.

be swamped however by the background from the uncoupled FM part. This scenario points to nanometer-coupled FE/FM multilayer stacks as appropriate candidates for enhancing the action of ME coupling.

In this study we present compelling evidence that magnetoelectric coupling is responsible for the above-mentioned asymmetry in the angular distribution of the FMR signal. Since the type of ME coupling is the key issue in composite multiferroics, we provide here a full quantitative analysis allowing to state that: (i) Particularly for the interface of $Co/BaTiO_3$ the type of the ME coupling is linear in **P** and **M**, (ii) it originates from the spin-dependent screening and not from strain effects, and (iii) angular-resolved FMR yields information on the symmetry of $\lambda_n(\mathbf{PM})^n$ and the strength of λ_n, whereas FMR itself only provides access to the strength of λ_n. Here λ_n, **P**, **M**, and n are the ME-coupling parameter, the polarization of the FE phase, the magnetization of the FM phase, and the order of ME interaction as given by a positive integer number, respectively. As an extension of previous experimental studies [24] we propose, based on theoretical results, that the FMR asymmetry can be tuned by an external static electric field. Equations are presented which relate the FMR asymmetry to the ME-coupling parameter λ_n and the polarization **P**.

II. GENERAL CONSIDERATIONS

Let us concentrate on a specific $Co/BaTiO_3$ composite (as employed, e.g., in Ref. [24]) and identify first the terms contributing significantly to the magnetic anisotropy. To do so it is important to characterize the crystallinity of the Co film. The transmission electron microscopy (TEM) of the sample reveals [24] a random spatial distribution of the orientation of the c axis in Co. The c-axis orientation varies on a nanometer scale, without any clear preferential orientation. Thus, the Co film can be characterized as a nanocrystalline material of hcp crystallites, without any pronounced texture.

The small size of the individual nanocrystallites in the low nanometer range leads to an isotropic magnetic crystalline anisotropy. This expectation follows from the larger magnitude of the exchange length of hcp Co as compared to the small crystallite size. The exchange length [28] is $l_{\rm ex} = \sqrt{A/K} = 8.7$ nm with the exchange constant $A = 31\ \mathrm{pJ\,m^{-1}}$ and the anisotropy constant $K = 0.4\ \mathrm{MJ\,m^{-3}}$. It is smaller than the crystallite size of the Co film as deduced from the TEM analysis. The magnitude of the resulting effective magnetic crystalline anisotropy is vanishingly small. This is evident from the analysis of the effective magnetic anisotropy $K_{\rm eff}$ of nanocrystalline FM [28], $K_{\rm eff} = K^4 D^6 A^{-3} = 231\ \mathrm{Jm^{-3}}$ with the average crystallite size $D = 2.5$ nm. Thus, the effective magnetic crystalline anisotropy is reduced by more than 3 orders of magnitude as compared to its bulk crystalline value, and it can be safely disregarded in the treatment of the free energy of the system. The same holds true for so-called surface anisotropy terms as the films under investigation [24] are rather thick (40 nm), and surface effects are irrelevant in this thickness range. Note that although the magnetocrystalline anisotropy is negligible, the magnetoelastic anisotropy, which reflects the strain dependence of the magnetocrystalline anisotropy, is still active [29].

This appreciation of the nanocrystallinity of the sample renders the shape anisotropy $F_{\rm SHP} = 0.5\mu_0 M_{\rm S}^2 = 1.3 \times 10^6\ \mathrm{MJ\,m^{-3}}$, the Zeeman energy $-\mu_0\mathbf{HM}$, the magnetoelastic anisotropy $F_{\rm MLT}$, and the magnetoelectric coupling $F_{\rm ME}$ as the only relevant contributions to the free energy of the system where the film magnetization is given by **M** and the external magnetic field by $\mu_0\mathbf{H}$.

In the following we will address the following questions: (1) What is the driving force for the reported remanent magnetization along the sample normal? (2) How can we understand the observation of the asymmetry of resonance fields in FMR for the magnetization being parallel or antiparallel to the sample normal?

To answer question (1) we need to consider the difference in free energy for the magnetization in plane (IP) as compared to the magnetization out of plane (OOP) where a positive value favors magnetization out of plane. We obtain for a constant polarization of the FE component along the $+z$ axis (out of plane),

$$F(M_{\rm IP}) - F(M_{\rm OOP}) = -0.5\mu_0 M_{\rm S}^2 + \sigma(\lambda_\parallel - \lambda_\perp) - \lambda_{\rm n}(P_z M_z)^n. \quad (1)$$

Here we introduce the magnetostrictive strains along the sample magnetization direction $\lambda_\parallel$ and perpendicular to it $\lambda_\perp$. The film stress is given by σ, and it is oriented within the film plane. It reflects growth-induced film stress. We have $\lambda_\parallel = \frac{2}{5}\lambda_{\rm A} + \frac{8}{15}\lambda_{\rm D} = -0.000\,071$, and $\lambda_\perp = \frac{2}{15}\lambda_{\rm A} + \frac{1}{3}(\lambda_{\rm B} + \lambda_{\rm C}) - \frac{4}{15}\lambda_{\rm D} = -0.000\,071$ from the properly averaged magnetostriction constants $\lambda_{\rm i}$ of bulk hcp Co [29,30]. From Ref. [30] we have $\lambda_{\rm A} = -45 \times 10^{-6}$, $\lambda_{\rm B} = -95 \times 10^{-6}$, $\lambda_{\rm C} = +110 \times 10^{-6}$, and $\lambda_{\rm D-100} = -45 \times 10^{-6}$. This gives $F_{\rm MLT} = -97\sigma\cos^2\psi$ with σ in megapascals and ψ being the angle between **M** and the direction of σ. Thus, a compressive, i.e., negative, film stress favors an out-of-plane magnetization direction (i.e., $\psi = \pi/2$).

Also the magnetoelectric coupling contribution in first order ($n = 1$) to the free energy may favor an out-of-plane magnetization direction provided that the product $\lambda_1(P_z M_z)$ is negative.

With reference to the system studied here we conclude that the reported remanent out-of-plane magnetization implies that here $+\sigma(\lambda_{\parallel} - \lambda_{\perp}) - \lambda_{\rm n}(P_z M_z)^n > +0.5\mu_0 M_{\rm S}^2$.

To address point (2) we need to consider those contributions to the free energy which are an odd function of the magnetization direction. This is required to obtain a different system response for magnetization along $+z$ as compared to magnetization along the $-z$ direction, where z is oriented out of plane, along the sample normal. Magnetoelastic coupling, which is the driving force behind magnetostriction [31], is an even function of the magnetization direction as evidenced by the quadratic dependence on the direction cosine α_i of the magnetization direction with respect to the sample axes [30,31]. Thus, magnetoelastic effects cannot be held responsible for the observed asymmetry of the resonance fields in FMR. This identifies the magnetoelectric coupling as the driving force behind the reported asymmetry in resonance fields.

In order to better understand the underlying physics and to properly interpret the experimental results we focus first on the approximation of a homogeneously magnetized FM denoted by the magnetization $\mathbf{M}$ and a uniformly polarized FE with polarization $\mathbf{P}$. In the following we lift the assumption of a negligible magnitude of the uniaxial magnetic anisotropy to also tackle more general cases.

The free energy for the thin FM film with total magnetization $\mathbf{M} = M_{\rm S}\{\cos\phi\ \sin\theta, \sin\phi\ \sin\theta, \cos\theta\}$ and the strength of the uniaxial anisotropy K_1 in external magnetic field $\mathbf{B} = B\{\sin\theta_{\rm B}, 0, \cos\theta_{\rm B}\}$ [Fig. 2(a)] coupled to a single-crystal-like polarization $\mathbf{P} = P_{\rm S}\{0,0,1\}$ has the form

$$F_{\rm FM} = -K_1(\sin^2\theta\ \cos^2\phi\ \sin^2\theta_{\rm u} + \cos^2\theta\ \cos^2\theta_{\rm u}) - \frac{K_1}{2}\sin 2\theta\ \sin 2\theta_{\rm u}\cos\phi - \left(\frac{K_{\rm S}}{d_{\rm FM}} - \frac{\mu_0 M_{\rm S}^2}{2}\right)\cos^2\theta - \mathbf{M}\cdot\mathbf{B} - \frac{3}{2}\lambda_{\rm MS}\sigma\ \cos^2\psi + \lambda_n(\mathbf{P}\cdot\mathbf{M})^n. \quad (2)$$

Here the terms containing K_1 represent a uniaxial magnetocrystalline anisotropy, leading to an easy axis direction tilted by the angle $\theta_{\rm u}$ in the xz plane, $K_{\rm S}$ describes magnetic surface anisotropy contributions which are significant for relatively low film thicknesses $d_{\rm FM}$ where a positive value favors magnetization out of the xy plane (Fig. 1). The term containing $\mu_0 M_{\rm S}^2$ denotes the demagnetizing field contributions, which favor a magnetization in plane. $\mathbf{M}\cdot\mathbf{B}$ considers the Zeemann interaction, and $\lambda_{\rm MS}$ and σ stand for magnetostrictive constant and the tensile stress, respectively. Finally, the last term, which originates from the interfacial electrostatic screening [32,33] and which is written in form of an expansion with respect to polarization and magnetization, takes into account the ME coupling.

Equation (2) alters after simplifications to

$$F_{\rm FM} = -K_1(\sin^2\theta\ \cos^2\phi\ \sin^2\theta_{\rm u} + \cos^2\theta\cos^2\theta_{\rm u}) - \frac{K_1}{2}\sin 2\theta\ \sin 2\theta_{\rm u}\cos\phi - \left(\frac{K_{\rm S}}{d_{\rm FM}} - \frac{\mu_0 M_{\rm S}^2}{2}\right)\cos^2\theta - M_{\rm S}B[\sin\theta\ \sin\theta_{\rm B}\cos(\phi-\phi_{\rm B}) + \cos\theta\ \cos\theta_{\rm B}] - \frac{3}{2}\lambda_{\rm MS}\sigma\ \cos^2\psi + \lambda_n P_z^n M_{\rm S}^n\cos^n\theta. \quad (3)$$

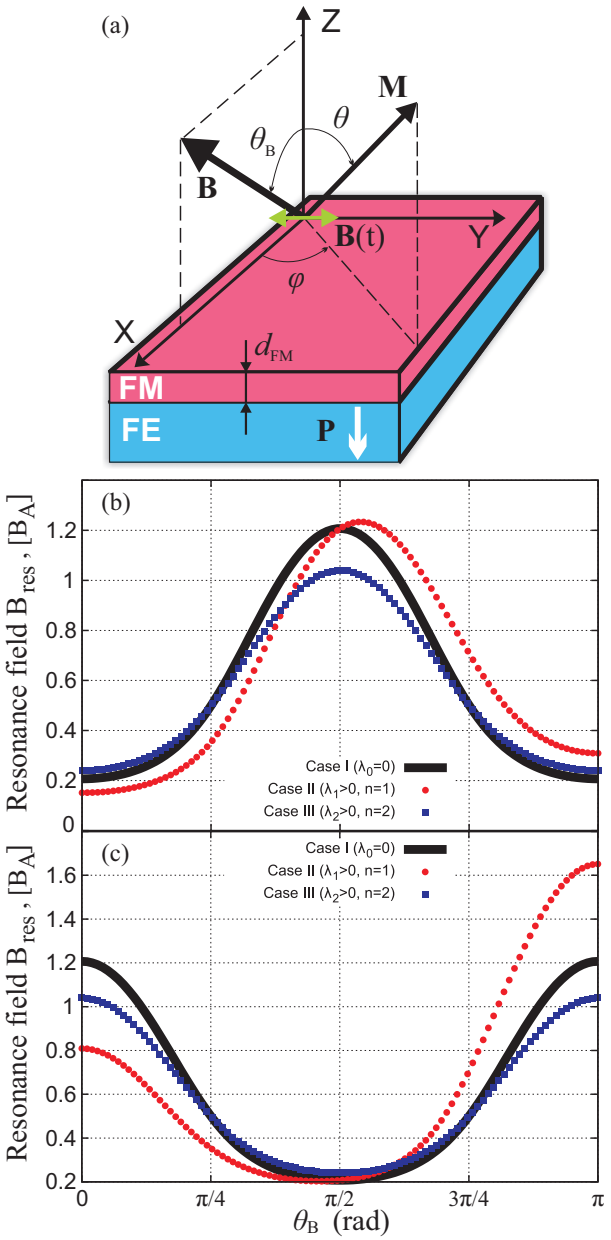

FIG. 2. (Color online) (a) Schematic of the plane of variation for the static magnetic field $\mathbf{B}$ and the magnetization $\mathbf{M}$. (b) Angular dependence of the positions of resonance fields based on Eqs. (6)–(8) in the case of an ultrathin FM film such that $K_{\rm S}/d_{\rm FM} \approx \mu_0 M_{\rm S}^2/2$ and therefore $K_{\rm eff} = K_1$ for different cases: I–III. (c) Angular dependence of the positions of resonance fields based on Eqs. (6)–(8) in the case of a nanometer-sized FM film such that $K_{\rm S}/d_{\rm FM} \approx 0$ and the demagnetizing contribution $\mu_0 M_{\rm S}^2/2$ becomes dominant, i.e., $K_{\rm eff} = -\mu_0 M_{\rm S}^2/2$ for different cases: I–III. Case I represents the situation without ME coupling, resulting in a fully symmetric angular dependence (b) and (c). Cases II and III demonstrate the changes in response of the homogeneously magnetized sample for different types of ME coupling with powers $n = 1$ and $n = 2$, respectively. Remarkable asymmetry can only be observed in the case of a linear ME coupling [case II, both (b) and (c)]. For a biquadratic ME coupling the angular dependence changes the strength of $B_{\rm res}$ shifts with no visible asymmetry (b) and (c). The fields are expressed in units of the anisotropy field $B_{\rm A} = 2K_1/M_{\rm S}$, $\omega/\gamma = B_{\rm A}$. Polarization is along the $-z$ direction, $P_z < 0$.

In Eq. (3) n can take the values 1,2, ... The conditions for the ferromagnetic resonance include the frequency of the rf-field ω and can be found from the equations known from literature [34–37] in the limit of low FM damping ($\alpha_{FM} \ll 1$),

$$\left(\frac{\omega}{\gamma}\right)^2 = \frac{1}{M_S^2 \sin^2\theta}\left[\frac{\partial^2 F}{\partial\phi^2}\frac{\partial^2 F}{\partial\theta^2} - \left(\frac{\partial^2 F}{\partial\phi\,\partial\theta}\right)^2\right]. \quad (4)$$

In what follows we will analyze each term of Eq. (3) separately in light of the experimentally observed FMR asymmetry in resonance fields.

III. ANALYTICAL RESULTS

A. Role of the ME coupling

First, we inspect the influence of the ME-coupling terms on the angular dependence of the resonance positions. For simplicity we disregard magnetostrictive effects ($\sigma = 0$) and align the easy axis along the z axis ($\theta_u = 0$). Under these assumptions one can denote $K_{eff} = K_1 + \frac{K_S}{d_{FM}} - \frac{\mu_0 M_S^2}{2}$.

For the bulk parameters of Co ($M_S = 1.44 \times 10^6$ A/m, $K_1 = 4.1 \times 10^5$ J/m^3, and $K_S \approx 10^{-3}$ J/m^2 Ref. [38], p. 271) the same calculations yield $\frac{\mu_0 M_S^2}{2} \approx 1.3 \times 10^6$ J/m^3, which can be balanced for an ultrathin Co film ($d_{FM} \approx 1$ nm) when $K_S/d_{FM} \approx 10^6$ J/m^3.

Depending on the thickness, i.e., the dominance of the $K_{eff}(d_{FM})$, the dependence of $B_{res}(\theta_B)$ will have the form either of Fig. 2(b) ($K_{eff} \approx K_1$) or of Fig. 2(c) ($K_{eff} \approx -\mu_0 M_S^2/2$).

Case I (No ME coupling, $\lambda_0 = 0$)

We can align the static magnetic field for simplicity such that $\phi_B = 0$ implying that $\phi \ll \pi$ ($\cos\phi \approx 1$, $\sin\phi \approx 0$). In addition, at resonances $\theta \approx \theta_B$ and $B = B_{res}$, therefore, from Eqs. (3) and (4) we find

$$\left(\frac{\omega}{\gamma}\right)^2 = \frac{1}{M_S^2 \sin^2\theta_B}[M_S B_{res}\sin^2\theta_B \times (2K_{eff}\cos 2\theta_B + M_S B_{res})]. \quad (5)$$

From Eq. (5) we find

$$B_{res} = -\frac{K_{eff}}{M_S}\cos 2\theta_B \pm \sqrt{\left(\frac{K_{eff}}{M_S}\right)^2 \cos^2 2\theta_B + \left(\frac{\omega}{\gamma}\right)^2}, \quad (6)$$

which is illustrated for the plus sign as $B_{res}(\theta_B)$ by the solid thick black curve in Figs. 2(b) and 2(c).

Case II (Linear ME coupling, $\lambda_1 \neq 0$, $n = 1$)

For the same conditions of resonances, of the alignment of the static magnetic field, and for the tetragonal phase of the FE polarization, which is aligned along the Z axis ($\phi_0 = 0$, $\theta_0 = 0$) we find

$$B_{res} = -\left(\frac{K_{eff}}{M_S}\cos 2\theta_B - \frac{\lambda_1 P_z}{2}\cos\theta_B\right) \pm \sqrt{\left(\frac{K_{eff}}{M_S}\cos 2\theta_B - \frac{\lambda_1 P_z}{2}\cos\theta_B\right)^2 + \left(\frac{\omega}{\gamma}\right)^2}, \quad (7)$$

which is plotted as $B_{res}(\theta_B)$ in Figs. 2(b) and 2(c) by the solid red circles.

Case III (biquadratic ME coupling, $\lambda_2 \neq 0$, $n = 2$)

Under the same conditions we derive

$$B_{res} = -\left(\frac{K_{eff}}{M_S} - \lambda_2 P_z^2 M_S\right)\cos 2\theta_B \pm \sqrt{\left(\frac{K_{eff}}{M_S} - \lambda_2 P_z^2 M_S\right)^2 \cos^2 2\theta_B + \left(\frac{\omega}{\gamma}\right)^2}, \quad (8)$$

which is shown as $B_{res}(\theta_B)$ in Figs. 2(b) and 2(c) by the solid blue squares.

B. Role of nonaxially symmetric terms

In the case of an ultrathin FM film with uniaxial magnetic anisotropy ($K_{eff} = K_1$) and if the easy axis forms an angle θ_u with the z axis, however, in the xz plane (Fig. 1), the free energy [Eq. (2)] reads

$$F_{FM} = -K_1(\sin^2\theta\cos^2\phi\sin^2\theta_u + \cos^2\theta\cos^2\theta_u) - \frac{K_1}{2}\sin 2\theta\sin 2\theta_u\cos\phi - \mathbf{M}\cdot\mathbf{B} + \lambda_n(\mathbf{P}\cdot\mathbf{M})^n. \quad (9)$$

Repeating the same steps as above and inserting the corresponding derivatives into Eq. (4), we obtain for the angular dependence of the resonance positions, first when $\lambda_n = 0$,

$$B_{res} = -\frac{K_1}{M_S} f_+(\theta_u,\theta_B) \pm \sqrt{\left(\frac{K_1}{M_S}\right)^2 f_-^2(\theta_u,\theta_B) + \left(\frac{\omega}{\gamma}\right)^2}, \quad (10)$$

where the notation $f_\pm(\theta_u,\theta_B) = \frac{\sin\theta_u}{\sin\theta_B}\cos(\theta_B - \theta_u) \pm \cos 2(\theta_B - \theta_u)$ is used. The angular dependence in the case of θ_u variation is shown in Fig. 3 from which a growing asymmetry is evidenced upon increasing the angle of the uniaxial anisotropy. However, as revealed from Fig. 3, the asymmetry exhibits an exactly opposite behavior for $\theta_u < \pi/2$ and for $\pi/2 < \theta_u < \pi$, which, if summed up (to mimic a polycrystalline sample with random orientation of larger crystallites as compared to the sample described in Ref. [24]), results in no total asymmetry.

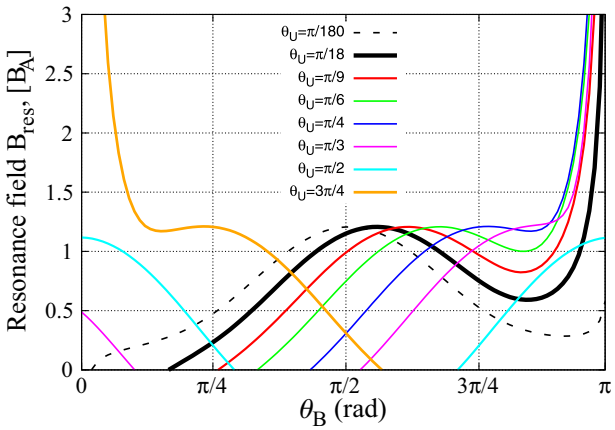

FIG. 3. (Color online) Angular dependence of the positions of resonance fields based on Eq. (10) for different values of the uniaxial anisotropy angle θ_u, which is varied in the xz plane as to simulate the situation of a polycrystalline magnetic sample. The fields are expressed in units of the anisotropy field $B_A = 2K_1/M_S$, $\omega/\gamma = B_A$. Azimuthal angles ϕ, ϕ_u and ϕ_B were set to zero.

IV. NUMERICAL RESULTS

Now we consider an interface consisting of $N_{\rm FE}$ FE coarse-grained polarization sites with the Ginzburg-Landau-Devonshire potential $F_{\rm FE}=\sum_{i=1}^{N_{\rm FE}}[\frac{\alpha_{\rm FE}}{2}P_{zi}^2+\frac{\beta_{\rm FE}}{4}P_{zi}^4+\frac{\kappa_{\rm FE}}{2}(P_{zi+1}-P_{zi})^2-P_{zi}E_z]$ corresponding to the tetragonal phase of $BaTiO_3$ [39], which is coupled via the linear ME-coupling term $\lambda_1\mathbf{P}_1\cdot\mathbf{M}_1$ to $N_{\rm FM}$ coarse-grained FM cells with the total free energy reading $F_{\rm FM}=\sum_{j=1}^{N_{\rm FM}}[-\frac{A}{a_{\rm FM}^2M_{\rm S}^2}\mathbf{M}_j\cdot\mathbf{M}_{j+1}-\frac{1}{M_{\rm S}^2}(K_1+\frac{K_{\rm S}}{a_{\rm FM}N_{\rm FM}}-\frac{\mu_0M_{\rm S}^2}{2})M_{zj}^2-\mathbf{M}_j\cdot\mathbf{B}_\Sigma(t)]$ (details of the parameters and the notations are given in Ref. [39]). Within this approach a nonuniform magnetization dynamics and associated with it finite-size effects are taken into consideration as to supplement the analytical results from the previous section.

The dynamical response is obtained using the set of the coupled Landau-Lifshitz-Gilbert equations for $\mathbf{M}_j(t)$ and the Landau-Khalatnikov equations for $\mathbf{P}_i(t)$ [40], whereas the response is calculated after reaching an equilibrium related to the magnetization relaxation time, which is inversely proportional to the magnetization damping $\alpha_{\rm FM}$.

The procedure of obtaining the FMR angular dependence is as follows: First, for each value of angle $\theta_{\rm B}$ of the applied external static magnetic field (Fig. 1), an FMR spectrum is calculated from which a maximum of the absorbed power and the corresponding resonance field $B_{\rm res}$ is detected as has been explained in Ref. [39] for $Fe/BaTiO_3$, albeit when dealing with Co possessing significantly stronger magnetocrystalline anisotropy as compared to the sample of Ref. [24], we decided for higher-frequency 35 GHz to resolve a maximum of absorption in the corresponding frame of static fields. This is followed by plotting the values of $B_{\rm res}$ as a function of the angle of the static magnetic field $\theta_{\rm B}$ for different values of the ME-coupling parameter (Fig. 4). As expected, the asymmetry $\Delta B_{\rm res}$ growths linearly with the strength of the ME coupling. Noteworthy is also the fact of the positively obtained asymmetry $\Delta B_{\rm res}$, which is explained by the negatively aligned entire FE polarization [cf. Eq. (7)]. On the contrary, in the experiment of Ref. [24] (Fig. 4) the FE polarization was positively aligned, resulting thus in a negative $\Delta B_{\rm res}$. Since the $B_{\rm res}(\theta_{\rm B})$ dependence resembles in a way an anisotropy profile, the state with $P_z<0$ for $\theta_{\rm B}=0$ is clearly more favorable than the state for $\theta_{\rm B}=\pi$ for the chosen ME-coupling energy.

The exact analytical form of the FMR asymmetry follows from the definition $\Delta B_{\rm res}=B_{\rm res}(\theta_{\rm B}=\pi)-B_{\rm res}(\theta_{\rm B}=0)$ and Eq. (7),

$$\Delta B_{\rm res}=-\lambda_1P_z+\sqrt{\left(\frac{K_{\rm eff}}{M_{\rm S}}+\frac{\lambda_1P_z}{2}\right)^2+\left(\frac{\omega}{\gamma}\right)^2}-\sqrt{\left(\frac{K_{\rm eff}}{M_{\rm S}}-\frac{\lambda_1P_z}{2}\right)^2+\left(\frac{\omega}{\gamma}\right)^2}. \quad (11)$$

Taking into account the typical values of the terms entering expression (11), $\omega/\gamma\approx1.24$ T, $|K_{\rm eff}|/M_{\rm S}\approx0.35$ T and $\lambda_1P_z/2\approx0.02$ T, one can expand the square roots of Eq. (11) and find a simplified expression for the FMR asymmetry,

$$\Delta B_{\rm res}\approx-\lambda_1P_z\left(1-\frac{K_{\rm eff}}{M_{\rm S}}\frac{1}{\omega/\gamma}\right). \quad (12)$$

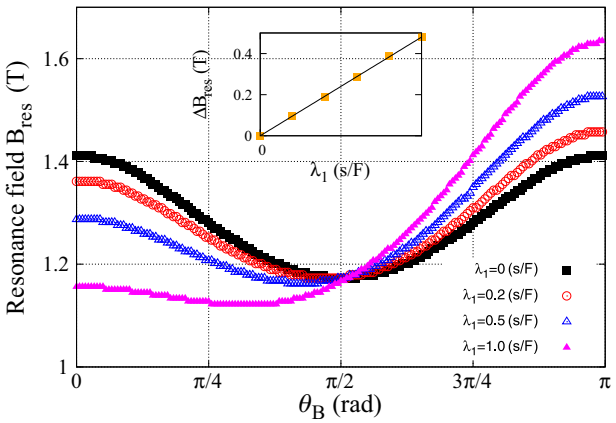

FIG. 4. (Color online) Numerically calculated angular dependence of the positions of resonance fields for angles $\theta_{\rm B}$ varied in the xz plane for different values of the ME coupling for $Co/BaTiO_3$. $\Delta B_{\rm res}=B_{\rm res}(\theta_{\rm B}=\pi)-B_{\rm res}(\theta_{\rm B}=0)$. Further parameters: $\omega/(2\pi)=35$ GHz, uniaxial anisotropy constant of Co $K_1=4.1\times10^5$ J/m^3, $\theta_{\rm u}=0$, $M_{\rm S}=1.44\times10^6$ A/m, $\alpha_{\rm FM}=0.1$, $d_{\rm FE}=8$, $d_{\rm FM}=1.3$ nm, and $\lambda_{\rm MS}=0$. No external electric field is applied, and the polarization is kept negative $P_z<0$. The inset shows the dependence of the asymmetry $\Delta B_{\rm res}$ on λ_1 (orange squares) and a linear fit $\Delta B_{\rm res}(\lambda_1)$ (black line).

For a fixed λ_1 the thickness dependence of the FMR asymmetry is inspected in Fig. 5; this effect which was not reported in Ref. [24]. The numerically calculated asymmetry (inset of Fig. 5) clearly demonstrates a reciprocal dependence on the FM thickness, which is a consequence of the localized character of

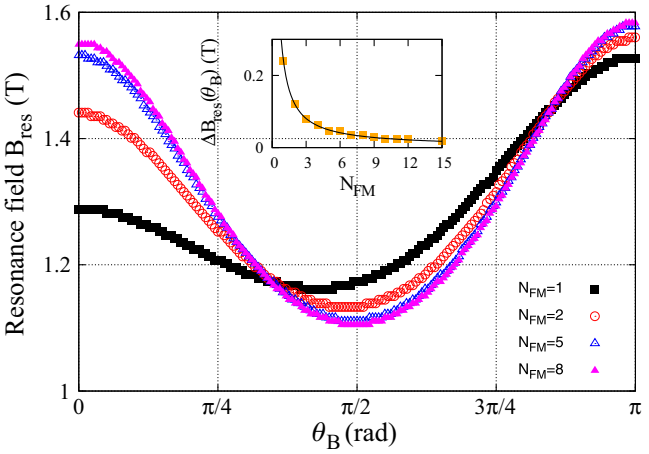

FIG. 5. (Color online) Numerically calculated angular dependence of the positions of resonance fields for angles $\theta_{\rm B}$ for various FM thicknesses $N_{\rm FM}=d_{\rm FM}/a_{\rm FM}$ varied in the xz plane for different values of the ME coupling for $Co/BaTiO_3$. $\Delta B_{\rm res}=B_{\rm res}(\theta_{\rm B}=\pi)-B_{\rm res}(\theta_{\rm B}=0)$. Further parameters: $\omega/(2\pi)=35$ GHz, the strength of the ME coupling $\lambda_1=0.5$ s/F, uniaxial anisotropy constant of Co $K_1=4.1\times10^5$ J/m^3, $\theta_{\rm u}=0$, $M_{\rm S}=1.44\times10^6$ A/m, $\alpha_{\rm FM}=0.1$, $d_{\rm FE}=8$, $a_{\rm FM}=1.3$ nm, and $\lambda_{\rm MS}=0$. No external electric field is applied, and the polarization is kept negative $P_z<0$. The inset represents the dependence of the FMR asymmetry on the thickness of the FM sample (orange squares) which was fitted by the $\Delta B_{\rm res}(N_{\rm FM})=0.237$ (T)$/N_{\rm FM}$ function (black solid curve).

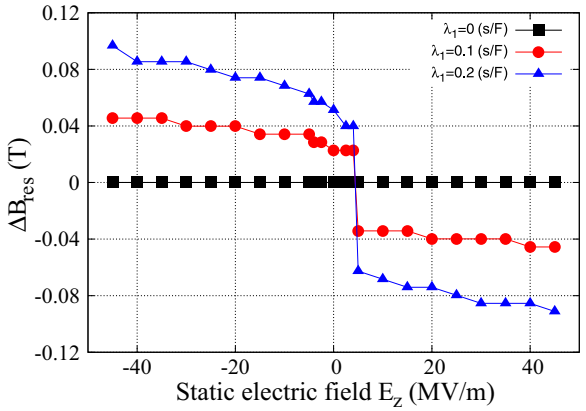

FIG. 6. (Color online) Numerically calculated FMR-asymmetry $\Delta B_{\rm res} = B_{\rm res}(\theta_{\rm B} = \pi) - B_{\rm res}(\theta_{\rm B} = 0)$ as a function of applied electric field E_z applied along the z axis. Further parameters: $\omega/(2\pi) = 35$ GHz, uniaxial anisotropy constant of Co $K_1 = 4.1 \times 10^5$ J/m^3, $\theta_{\rm u} = 0$, $M_{\rm S} = 1.44 \times 10^6$ A/m, $\alpha_{\rm FM} = 0.1$, $d_{\rm FE} = 8$, $d_{\rm FM} = 2.6$ nm, and $\lambda_{\rm MS} = 0$.

the charge-mediated ME coupling, suggesting for the thickness dependence $\Delta B_{\rm res} \approx -\lambda_1 P_z(1 - \frac{K_{\rm eff}}{M_{\rm S}} \frac{1}{\omega/\gamma})\lambda_{\rm m}/d_{\rm FM}$, where $\lambda_{\rm m}$ denotes the spin diffusion length of the FM. We note, that according to Eq. (12) a dependence on thickness also enters the effective anisotropy $K_{\rm eff}$, which can be eliminated by, e.g., measurements at different rf frequencies ω. Moreover, the results of Fig. 5 (inset) imply that the measured ME-coupling strength for a 40-nm-thick Co layer (Ref. [24], Fig. 4) could have significantly higher values for thinner Co layers.

Although Eq. (7) can be used for calculation of the FMR asymmetry as a function of the FE polarization, its dependence on the external static electric field is not straightforward since the polarization is in general a nonlinear function of the E field. For this reason we numerically model the influence of the electric static field on the FMR asymmetry $\Delta B_{\rm res}$, illustrated in Fig. 6. As a reference we show the $\lambda_1 = 0$ case, which, as expected, is fully symmetric. Upon increasing the electric field E_z from the negative to the positive area, we witness an abrupt change in $\Delta B_{\rm res}$, which is a signature of the FE $BaTiO_3$ and is associated with a switching of the FE polarization [change in sign in Eq. (12)]. This observation was previously reported for the original FMR spectra for the interface of $Fe/BaTiO_3$ (Fig. 2 of Ref. [39]). The point of the sign change in $\Delta B_{\rm res}(E_z)$ is related to the height of the FE barrier. It goes without saying that the obtained $\Delta B_{\rm res}(E_z)$ dependence is also asymmetric with respect to the applied electric field. Interestingly, a similar behavior has recently been observed in the experiments performed for permalloy/PMN-PT [Fig. 2(b)], Ref. [25]. As discussed in Ref. [26], for this system a linear magnetoelectric coupling is appropriate.

V. DISCUSSION

Based on Eqs. (2)–(8) we interpret the asymmetry of $B_{\rm res}(\theta_{\rm B})$ reported in Ref. [24].

Magnetoelectric coupling. As inferred from Figs. 2(b) and 2(c) only the terms which are linear with respect to magnetization, e.g., $\lambda_1 \mathbf{P} \cdot \mathbf{M}$, cause asymmetry in the $B_{\rm res}(\theta_{\rm B})$ dependence, whereas the sign of the coupling $\pm\lambda$ can also be detected from the angular dependence. In particular, if the original coupling is positive, then the values of $B_{\rm res}(\theta_{\rm B} = \pi)$ are higher than those for $\theta_{\rm B} = 0$ [Figs. 2(b) and 2(c), red circles]. In Fig. 4 of Ref. [24] the shift/asymmetry is opposite implying rather a negative sign for the **M** contribution to the total free energy.

Additionally, as inferred from Figs. 4 and 5, the stronger the ME coupling, the larger the $\Delta B_{\rm res}$ shift, which, nevertheless, strongly decays upon increasing the FM thickness.

Exchange bias (EB). A hypothesis of the EB effect emerging from a possible oxidation of Co at the interface of $Co/BaTiO_3$ and resulting in a typical EB-energy contribution scaling according to $\mu_0 \mathbf{M} \cdot \mathbf{H}_{\rm EB}$ [41] to be responsible for the shifts [42] in Fig. 4 of Ref. [24] can be disproved by three facts. First, significant strong EB usually shows up for temperatures much lower than room temperature [41,43], whereas the measurements revealed by Fig. 4 of Ref. [24] were performed at $T = 300$ K. The pronounced temperature dependence of the EB effect is understood in terms of the formation of anti-FM coupling near the interface between CoO with the FM, exhibiting a superparamagnetic behavior at elevated temperatures [44]. Second, irrespective of the mono- or polycrystalline (Fig. 6 of Refs. [41,43]) structure of the crystal, a visible shift in the magnetic hysteresis should be detectable, which is not present both for in- and out-of-plane applied magnetic fields as evidenced from Fig. 3 of Ref. [24]. Finally, as reported earlier [41,43,45] the effect of EB always shows a pronounced thickness dependence, which results from the interface nature of the underlying coupling. None of the thickness-dependent measurements reported in Ref. [24] (Fig. 3) demonstrate any EB effect for further thicknesses (15 or 40 nm). In addition, the authors of Ref. [24] explicitly mention that "the same measurements performed with a polycrystalline Co film of equivalent thickness on top of a $TiO_2/Si(001)$ substrate have led to a perfectly symmetric resonance curve," which again disproves the idea that EB plays a role for the phenomena discussed here.

Another important issue mentioned in Ref. [24] concerns the connection of the FE polarization and the shift in the angular dependence, i.e., "Importantly, we have checked that the shifting of the resonance field between the two 0° and 180° orientations disappears when increasing the temperature from 300 to 390 K where the BTO layers transform into the paraelectric ($P_z = 0$) cubic phase."

Depolarizing fields and polycrystalline sample. The presence of depolarizing fields [46] enters into the free energy as $+\sum_\alpha N_\alpha \mu_0 M_\alpha^2$ terms (where $\alpha = x,y,z$ denotes the Cartesian components and N_α are known as demagnetizing factors [38,47]) might result in a correction of the uniaxial anisotropy strength K_1 in the final expression for the resonance fields when $\alpha = z$.

A polycrystalline structure generally has a strong impact on the magnetic properties of the sample [38,48], such as the hysteresis curve, the response, and the switching properties. FM polycrystals can be modeled as a sum of interacting crystallites [49], whereas the three principal contributions in expression (2) should be substituted by the corresponding sums, e.g., $\sum_i K_{1i} \cos^2 \theta_i$ (i numbers polycrystallites within the polycrystal). As a result, the positions of the resonances

are expected to be shifted to stronger fields (due to interaction between the polycrystallites), and the FMR spectra themselves should show visible broadening, known, e.g., for weakly interacting nanoparticles with randomly oriented anisotropy axes [50]. The direct influence on the asymmetry of $B_{\rm res}(\theta_{\rm B})$ is observed as revealed by Fig. 3.

Ferromagnetic domains. The effect of a multidomain structure on the resonance-field behavior was studied in detail in Ref. [51]. It was shown, that depending on the geometry of the sample, the type of the anisotropy and the thickness of the sample, the appearance of two (several) additional peaks in FMR is ascribed to a multidomain structure.

VI. CONCLUSIONS

Using formulas based on the expressions from Refs. [35,36] for the positions of FMR [Eq. (4)] and on numerical formalism based on the propagation of the coupled polarization/magnetization dynamics we strived to support the results of Ref. [24] stressing the dominance of the screening charge contribution to the ME coupling at the interface of the polycrystalline Co layer with the single-crystal $BaTiO_3$ thin film. We emphasize that for the case of a FM layer coupled to a FE substrate, it is the linear $\mathbf{P}\cdot\mathbf{M}$ term describing the ME coupling that gives rise to the experimentally observed asymmetry of the positions of resonance. Other contributions, such as nonaxially symmetric magnetocrystalline anisotropies (Fig. 3), magnetostriction, or exchange bias effects do not contribute to the asymmetry. Higher odd order ME coupling may in principle result in an asymmetry of FMR angular dependence; these ME terms are, however, usually substantially weaker than the linear ME coupling (i.e., $\lambda_1 \gg \lambda_{2n+1}$ for $n > 0$).

As a measure for the strength of the ME coupling one might define a difference of the resonance fields $\Delta B_{\rm res}$ for anti- and parallel orientations of the magnetic static field B with respect to the FM normal (cf. Fig. 1). Only in the case of the linear ME coupling does one obtain a nonzero expression similar to Eq. (11) or as in the case of a weak ME coupling—a simplified version [Eq. (12)]. As follows from expression (12), the asymmetry is sensitive to the orientation of the FE polarization ($\pm P_z$) and to the sign of the total anisotropy $K_{\rm eff}$, which depending on the FM thickness might be positive or negative. We note, that the asymmetry detected in the experiments of Ref. [24] was fully attributed to the ME coupling λ_1, however, as follows from Eq. (12), it also involves the rf-frequency and anisotropy corrections. The thickness dependence of the FMR asymmetry has two contributions: One originates from a localized character of the ME coupling acting over the so-called spin diffusion length $\lambda_{\rm m}$ and another, which is a consequence of the thickness dependence of the effective anisotropy $K_{\rm eff}$. The last contribution manifests itself only if $\lambda_1 \neq 0$.

We finally note that recent FMR experiments performed for an ultrathin permalloy/PMN-PT multiferroic interface [25] distinguished between strain- and charge-mediated ME contributions, yielding for the ME anisotropy due to the screening charge the values on the order of 0.01 T, which is at least one order of magnitude weaker than the ME anisotropy field 0.14 T reported in Ref. [24] and the value $\Delta B_{\rm res} = 0.14$ T calculated here for $\lambda_1 = 0.3$ s/F (cf. Fig. 4). The relatively high strength of ME coupling in $Co/BaTiO_3$ results in an induced effective magnetic field in the range of $\lambda_1 P_z = 0.3\ {\rm s/F} \times 0.268\ {\rm C/m^2} \approx 0.08$ T. As the FE polarization can be controlled by an external electric field, FMR should be observable in the presence of an applied static electric field only, i.e., even if the static magnetic field is zero ($B = 0$).

ACKNOWLEDGMENTS

The financial support through Projects SFB 762 of the German Research Foundation and the National Natural Science Foundation of China (Projects No. 11104123 and No. 11474138) are gratefully acknowledged. The authors thank P. Borisov for valuable discussions on exchange bias.

[1] M. Fiebig, J. Phys. D: Appl. Phys. **38**, R123 (2005).
[2] W. Eerenstein, N. D. Mathur, and J. F. Scott, Nature (London) **442**, 759 (2006).
[3] R. Ramesh and N. A. Spaldin, Nature Mater. **6**, 21 (2007).
[4] C.-W. Nan, M. I. Bichurin, S.-X. Dong, D. Viehland, and G. Srinivasan, J. Appl. Phys. **103**, 031101 (2008).
[5] V. Garcia, M. Bibes, L. Bocher, S. Valencia, F. Kronast, A. Crassous, X. Moya, S. Enouz-Vedrenne, A. Gloter, D. Imhoff, C. Deranlot, N. D. Mathur, S. Fusil, K. Bouzehouane, and A. Barthélémy, Science **327**, 1106 (2010).
[6] H. L. Meyerheim, F. Klimenta, A. Ernst, K. Mohseni, S. Ostanin, M. Fechner, S. Parihar, I. V. Maznichenko, I. Mertig, and J. Kirschner, Phys. Rev. Lett. **106**, 087203 (2011).
[7] D. Pantel, S. Goetze, D. Hesse, and M. Alexe, Nature Mater. **11**, 289 (2012).
[8] N. Lei, T. Devolder, G. Agnus, P. Aubert, L. Daniel, J.-V. Kim, W. Zhao, T. Trypiniotis, R. P. Cowburn, C. Chappert, D. Ravelosona, and P. Lecoeur, Nat. Commun. **4**, 1378 (2013).
[9] R. O. Cherifi, V. Ivanovskaya, L. C. Phillips, A. Zobelli, I. C. Infante, E. Jacquet, V. Garcia, S. Fusil, P. R. Briddon, N. Guiblin, A. Mougin, A. A. Ünal, F. Kronast, S. Valenica, B. Dkhil, A. Barthélémy, and M. Bibes, Nature Mater. **13**, 345 (2014).
[10] G. Bertotti, I. D. Mayergoyz, and C. Serpico, *Nonlinear Magnetization Dynamics* (Elsevier, Amsterdam, 2009).
[11] M. Bauer, J. Fassbender, B. Hillebrands, and R. L. Stamps, Phys. Rev. B **61**, 3410 (2000).
[12] T. Gerrits, H. A. M. van den Berg, J. Hohlfeld, L. Bär, and T. Rasing, Nature (London) **418**, 509 (2002).
[13] J. C. Slonczewski, J. Magn. Magn. Mater. **159**, L1 (1996).
[14] L. Berger, Phys. Rev. B **54**, 9353 (1996).
[15] J. A. Katine, F. J. Albert, R. A. Buhrman, E. B. Myers, and D. C. Ralph, Phys. Rev. Lett. **84**, 3149 (2000).
[16] M. D. Stiles and A. Zangwill, Phys. Rev. B **66**, 014407 (2002).
[17] Y. Tserkovnyak, A. Brataas, and G. E. Bauer, J. Magn. Magn. Mater. **320**, 1282 (2008).
[18] D. Khomskii, Physics **2**, 20 (2009).

[19] M. I. Bichurin, V. M. Petrov, O. V. Ryabkov, S. V. Averkin, and G. Srinivasan, Phys. Rev. B **72**, 060408(R) (2005).
[20] K. J. A. Franke, D. López Gonález, S. J. Hämäläinen, and S. van Dijken, Phys. Rev. Lett. **112**, 017201 (2014).
[21] C. A. F. Vaz, J. Hoffman, Ch. A. Ahn, and R. Ramesh, Adv. Mater. **22**, 2900 (2010).
[22] C. A. F. Vaz, J. Phys.: Condens. Matter **24**, 333201 (2012).
[23] L. Chotorlishvili, R. Khomeriki, A. Sukhov, S. Ruffo, and J. Berakdar, Phys. Rev. Lett. **111**, 117202 (2013); A. Sukhov *et al.*, J. Phys. D: Appl. Phys. **47**, 155302 (2014).
[24] N. Jedrecy, H. J. von Bardeleben, V. Badjeck, D. Demaille, D. Stanescu, H. Magnan, and A. Barbier, Phys. Rev. B **88**, 121409(R) (2013).
[25] T. Nan, Z. Zhou, M. Liu, X. Yang, Y. Gao, B. A. Assaf, H. Lin, S. Velu, X. Wang, H. Luo, J. Chen, S. Akhtar, E. Hu, R. Rajiv, K. Krishnan, S. Sreedhar, D. Heiman, B. M. Howe, G. J. Brown, and N. X. Sun, Sci. Rep. **4**, 3688 (2014).
[26] C.-L. Jia, T.-L. Wei, C.-J. Jiang, D.-S. Xue, A. Sukhov, and J. Berakdar, Phys. Rev. B **90**, 054423 (2014).
[27] J. Bass and W. P. Pratt, Jr., J. Phys.: Condens. Matter **19**, 183201 (2007).
[28] G. Herzer, Phys. Scr. **T49**, 307 (1993).
[29] *Rapidly Quenched Metals*, edited by S. Steeb, H. Warlimont, R. C. O'Handley, and N. J. Gracy (Elsevier, Amsterdam, 1985), p. 1125.
[30] W. P. Mason, Phys. Rev. **96**, 302 (1954).
[31] D. Sander, Rep. Prog. Phys. **62**, 809 (1999).
[32] C.-G. Duan, S. S. Jaswal, and E. Y. Tsymbal, Phys. Rev. Lett. **97**, 047201 (2006).
[33] M. Fechner, I. V. Maznichenko, S. Ostanin, A. Ernst, J. Henk, P. Bruno, and I. Mertig, Phys. Rev. B **78**, 212406 (2008).
[34] Ch. Kittel, Phys. Rev. **73**, 155 (1948).
[35] H. Suhl, Phys. Rev. **97**, 555 (1955).
[36] J. Smit and H. G. Beljers, Philips Res. Rep. **10**, 113 (1955).
[37] S. V. Vonsovskii, *Ferromagnetic Resonance: The Phenomenon of Resonant Absorption of a High-Frequency Magnetic Field in Ferromagnetic Substances* (Pergamon, Oxford, 1966).
[38] J. M. D. Coey, *Magnetism and Magnetic Materials* (Cambridge University Press, Cambridge, UK, 2010).
[39] A. Sukhov, P. P. Horley, C.-L. Jia, and J. Berakdar, J. Appl. Phys. **113**, 013908 (2013).
[40] A. Sukhov, C.-L. Jia, P. P. Horley, and J. Berakdar, J. Phys.: Condens. Matter **22**, 352201 (2010); A. Sukhov *et al.*, Ferroelectrics **428**, 109 (2012); P. P. Horley, A. Sukhov, C.-L. Jia, E. Martínez, and J. Berakdar, Phys. Rev. B **85**, 054401 (2012); C.-L. Jia *et al.*, Europhys. Lett. **99**, 17004 (2012).
[41] J. Nogues and I. K. Schuller, J. Magn. Magn. Mater. **192**, 203 (1999).
[42] The effect of the asymmetry for the angular dependence of the resonance fields induced by the exchange bias effect is in general known and was previously reported in J. Geshev, L. G. Pereira, and J. E. Schmidt, Phys. Rev. B **64**, 184411 (2001).
[43] F. Radu, M. Etzkorn, R. Siebrecht, T. Schmitte, K. Westerholt, and H. Zabel, Phys. Rev. B **67**, 134409 (2003).
[44] M. D. Stiles and R. D. McMichael, Phys. Rev. B **60**, 12950 (1999).
[45] J. Nogues, J. Sort, V. Langlais, V. Skumryev, S. Surinach, J. S. Munoz, and M. D. Baro, Phys. Rep. **422**, 65 (2005).
[46] W. F. Brown, *Magnetostatic Principles in Ferromagnetism* (North-Holland, Amsterdam, 1962).
[47] S. Chikazumi, *Physics of Ferromagnetism* (Oxford University Press, New York, 2002).
[48] R. C. O'Handley, *Modern Magnetic Materials: Principles and Applications* (Wiley, New York, 2000).
[49] V. G. Masheva, J. N. Kotzev, and A. V. Apostolov, Appl. Phys. **23**, 93 (1980).
[50] A. Sukhov, K. D. Usadel, and U. Nowak, J. Magn. Magn. Mater. **320**, 31 (2008).
[51] J. O. Artman, Phys. Rev. **105**, 74 (1957).